APPLIED AND ENVIRONMENTAL MICROBIOLOGY, Mar. 1979, p. 480–486
0099-2240/79/03-0480/07$02.00/0

Vol. 37, No. 3

Degradation of Poliovirus by Adsorption on Inorganic Surfaces

JAMES P. MURRAY† AND STEVEN J. LABAND

Departments of Applied Earth Sciences and Medical Microbiology, Stanford University, Stanford, California 94305

Received for publication 18 December 1978

Alteration of the specific infectivity of ^{3}H-labeled ribonucleic acid and ^{14}C-protein labeled poliovirus type 1 by adsorption on inorganic surfaces is investigated by application of kinetic theory to data obtained from sequential extractions of adsorbed virus. Some surfaces, e.g., SiO_2, appear to have no significant effect. On the other hand, CuO substantially decreases the specific infectivity of adsorbed preparations. Differences in kinetic plots between ^{3}H-labeled ribonucleic acid and ^{14}C-labeled protein suggest that the inactivation observed involves physical disruption of virions. Van der Waals interactions between solid surfaces and virus are suspected to induce spontaneous virion disassembly. Surface catalyzed disassembly in aquatic and soil environments is implicated as an important mechanism controlling enterovirus dissemination. Methods developed here to evaluate complete recovery of adsorbed virus have potential application to other degradation studies and problems concerning virus recovery from adsorbents used in virus concentrators.

The problem of recovering virus adsorbed to various inorganic surfaces is widely recognized (6). The question then arises, is the virus merely strongly adsorbed, or is some fraction of the preparation inactivated by alteration of the virion structure? A method for calculating the amount of virus recoverable with an infinite number of extractions is developed. It involves applying kinetic theory to information obtained from sequential extractions of purified labeled virus. Comparing the recoverable amounts with amounts initially adsorbed provides definitive answers to our question.

MATERIALS AND METHODS

Virus and assay. Poliovirus type 1, strain LSc2ab, was propagated in HeLa cells and labeled with [5,6-^{3}H]uridine and ^{14}C-labeled amino acid mixture from New England Nuclear, in the presence of 1 μg of actinomycin D per ml. It was purified by differential ultracentrifugation, $C_2Cl_3F_3$ extraction, banding in sucrose and CsCl gradients, and exhaustive dialysis against pH 7, 0.02 ionic strength $NaHCO_3$ buffer containing NaCl (0.02 I buffer). This solution contained 1.093×10^{-2} M $NaHCO_3$ and 9.156×10^{-2} M NaCl equilibrated with 5% CO_2 in air. After purification, virus was filtered with 0.45 μm membrane filters (Millipore Corp.) and stored at 4°C. Cells were maintained and virus was assayed in Eagle minimal essential medium with Earle salts (Grand Island Biological Co.) augmented with 100 U of penicillin G per ml and 100 μg of streptomycin sulfate per ml plus 10% fetal bovine serum (Microbiological Associates). Infectivity was measured by the plaque assay of Dulbecco and Vogt adapted by McClain and Schwerdt (9). Serial dilutions were prepared in Hanks balanced salt solution plus 4% maintenance medium which was added to block virus adsorption to dilution tubes (2). Media and buffers were prepared with double-distilled deionized water (ddd H_2O).

Adsorbents. Five solids, α-SiO_2, α-Fe_2O_3, α-Al_2O_3, β-MnO_2, and CuO were selected for this investigation. SiO_2, Min-U-Sil 5, a gift of Pennsylvania Glass Sand Corp., was refluxed in aqua regia and 16 M HNO_3 overnight to remove metallic impurities, and extensively washed with ddd H_2O. Silica particles were <5 μm in diameter, and duplicate BET surface areas (1) were 5.19 and 5.49 m^2 per g. Other solids were ACS reagent powders and are characterized elsewhere (J. P. Murray and G. A. Parks, manuscript in preparation). They were sterilized by heating to 200°C for ≥2 h and stored dry. Structural forms, indicated by α, β prefixes, were confirmed by X-ray diffraction.

Adsorption of virus. Virus was adsorbed to the following quantities of solid: SiO_2—4.02 ± 0.01 g; Fe_2O_3, MnO_2, CuO—1.00 ± 0.01 g; and Al_2O_3—0.083 ± 0.0002 g. Adsorption was carried out in 15-ml sterile polyethylene scintillation vials containing solids and 10 ml of 0.02 I buffer. Duplicate samples were rotated at 15 ± 2°C and 1 rpm for 2- and 24-h incubation periods prior to eluting and analyzing for adsorbed virus.

Elution of virus from silica. After adsorption of virus to SiO_2 samples and incubation in 0.02 I buffer for 2- and 24-h periods, aliquots of solid-liquid mixtures were withdrawn for determining the amount of virus

† Present address: Interdisciplinary Programs in Health, Harvard School of Public Health, Boston, MA 02115.

remaining in the liquid phase. These aliquots were centrifuged at 15,000 rpm for 10 min in the 40.2 rotor of a Spinco model L ultracentrifuge and sampled for residual infectivity and radioactivity. The quantities of solid removed were determined by rinsing this pellet with ddd H_2O, drying at 200°C, and weighing.

The total adsorbed virus remaining in the reaction vessel (Ads_i) is:

$$Ads_i = \frac{w_r}{w_a}(Tot - C_u V_a) \quad (1)$$

where w_r is the weight of solid remaining in the vessel, w_a is the total weight of solid initially added, Tot is the total amount of virus initially added to the vial, determined from analysis of standards run in parallel, C_u is the virus concentration not initially adsorbed, and V_a is the volume of 0.02 I buffer left in the vial.

Immediately after withdrawing the aliquots mentioned above, 10× concentrated elution medium was added to the samples so as to bring the concentration of elution medium therein to ~1×. 10× elution medium contained the following: disodium ethylenediaminetetraacetate, 0.01 M; sodium dodecyl sulfate, 2% (wt/vol); glycine, 0.1 M; tryptone (Difco), 0.1%; and fetal bovine serum, 10% (vol/vol). It was adjusted to pH 12 with NaOH. Diluting 1:10 with 0.02 I buffer, in a manner comparable to desorption experiments but with no solid or virus present, reduced the pH to 9.8. The samples were then placed on a rotator for 1 h at 1 rpm and 25 ± 2°C, during which virus desorbed into the elution medium.

After elution, vials were clarified by centrifuging at 1,000 rpm for 5 min in a PR-2 refrigerated centrifuge from International Equipment Co., and aliquots were sampled for eluted virus after additional ultracentrifugation as mentioned above. The recovered virus (Ads_r) is:

$$Ads_r = C_e V_e - C_u V_r \quad (2)$$

where C_e is the concentration in the elution medium, V_e is its volume, and V_r is the residual volume of 0.02 I adsorption buffer left in the vial prior to adding concentrated elution medium.

The terms used for concentrations and total amounts in our expressions refer to either infectivity, ^{3}H-labeled ribonucleic acid (RNA), or ^{14}C-labeled protein data. Volumes were determined by pipetting known quantities or by weighing.

Elution from other solids. With other solids only small fractions of initially adsorbed radioactivity and infectivity could be recovered by single extractions. Multiple extraction techniques and kinetic theory are required for evaluating recoverable virus.

Virus was adsorbed as described with SiO_2 except that vials were centrifuged for 5 min at 1,000 rpm in the PR-2 refrigerated centrifuge after adsorption, and then residual buffer was sampled directly for infectivity. Buffers were then aspirated, and solids were resuspended in 10 ml of pH 8.8, 1× elution medium. This medium contained one-tenth all constituents listed for 10× medium plus 0.01 M $NaHCO_3$. Reaction vessels were rotated for 15 min at 25 ± 2°C and 1 rpm, centrifuged at 1,000 rpm in the PR-2 centrifuge for 5 min, and sampled for virus eluted. The remaining elution medium in the vial was then aspirated, and new elution medium was added. Extraction with elution medium was done four times in sequence at 30-min intervals. Volumes in reaction vessels were monitored throughout the experiment by pipetting and weighing.

Concentrations required for application of kinetic theory were evaluated by:

$$C'_n = C_n - C_{n-1} V_r \quad (3)$$

where C'_n is the concentration of virus desorbing from the solid during extraction n, C_n is the analyzed concentration in the elution medium after extraction n, and C_{n-1} is the analyzed concentration in the previous extraction.

Controls. Controls demonstrated the following: (i) buffers used during adsorption and dissolution products of the various adsorbents had no significant effect on the specific infectivity of the virus preparation for periods up to 24 h; (ii) reaction vessels did not adsorb measurable quantities of virus; (iii) elution media had no effect during appropriate incubation times on the virus titer; (iv) elution media had no effect on the HeLa cell assay system when diluted 1:30 with serial dilution medium; and (v) adsorption of virus to all solids tested did not occur in the presence of elution media.

RESULTS

Derivation of kinetic theory for multiple extractions. In this section, we will derive appropriate expressions required for calculation of the total amount of virus recoverable with an infinite number of extractions. For multiple extraction data, we can write the mass-balance expression:

$$Ads_{n-1} - Ads_n = C'_n V_n \quad (4)$$

where Ads_n is the total virus adsorbed after extraction n, C'_n is the virus concentration in the supernatant due to desorption during step n, and V_n is the supernatant volume. The subscript $n - 1$ refers to the previous extraction.

If the probability of adsorbate-adsorbate interactions is small, as suggested by low surface coverage, we can assume a first-order rate for the desorption reaction. Since we have no adsorption in the presence of elution medium, we can write:

$$\frac{dAds}{dt} = -kAds \quad (5)$$

where k is the rate constant and t represents elapsed time. This expression also assumes that $dk/dn \rightarrow 0$. This last assumption will be discussed in the following section.

Integrating equation 5 and substituting into equation 4 we have:

$$V_n C'_n = Ads_{n-1}[1 - \exp(-k\Delta t)] \quad (6)$$

and by rearranging:

$$C'_n = DAds_n \quad (7)$$

where $D = \exp[(k\Delta t) - 1]/V$. Substituting again into equation 4 we have:

$$C'_n - C'_{n-1} = C'_n DV_n. \quad (8)$$

Keeping V and Δt invariant with respect to n and treating our extractions as a continuous process, we can write:

$$\frac{dC'}{C'} = -DVdn. \quad (9)$$

Integrating this expression, we have:

$$\ln C' \Big|_0^x = -DVn \Big|_0^x \quad (10)$$

where x represents the sequence number of the final extraction.

Plotting ln C' against n will give a straight line with slope $-DV$ and intercept ln C'_o. The amount recoverable in an infinite number of extractions is then:

$$Ads_o = \frac{C'_o}{D} \quad (11)$$

by equation 7.

Recovery information and kinetic plots. If we recover all infectivity and radioactivity initially added, either by complete elution or by application of our extraction theory, we can say that specific virus infectivity is not reduced during adsorption. If we recover all radioactivity, but lose significant amounts of infectivity, we have conclusive evidence that virus is inactivated. This approach is still valid even if traces of labeled impurity are present in the original virus preparation.

The amounts of virus initially adsorbed to our surfaces and the amounts recovered are presented in Tables 1 to 5. Standard deviations about initial amounts are calculated from count-

TABLE 1. *Comparison of virus initially adsorbed (Ads_i) with virus recovered (Ads_r) for SiO_2*

Incubation time	Measurement[a]	Sample[b]	Ads_i	Ads_r
2 h	Infectivity (log PFU)	A	8.46 ± 0.19	8.71 ± 0.22
		B	8.41 ± 0.22	8.63 ± 0.25
	^{3}H-labeled RNA (log cpm)	A	3.22 ± 0.06	3.17 ± 0.08
		B	3.17 ± 0.07	3.12 ± 0.09
	^{14}C-labeled protein (log cpm)	A	3.20 ± 0.05	3.13 ± 0.07
		B	3.15 ± 0.06	3.13 ± 0.08
24 h	Infectivity (log PFU)	C	8.46 ± 0.22	8.14 ± 0.23
		D	8.49 ± 0.22	8.30 ± 0.20
	^{3}H-labeled RNA (log cpm)	C	3.41 ± 0.06	3.38 ± 0.08
		D	3.49 ± 0.05	3.56 ± 0.07
	^{14}C-labeled protein (log cpm)	C	2.29 ± 0.05	2.86 ± 0.07
		D	2.99 ± 0.05	2.96 ± 0.07

[a] Abbreviations: PFU, plaque-forming units; cpm, counts per minute.
[b] A, B and C, D are duplicates.

TABLE 2. *Comparison of virus initially adsorbed (Ads_i) on Fe_2O_3 with virus recovered by kinetic analysis of data from four extractions (Ads_o)*

Incubation time	Measurement[a]	Sample[b]	Ads_i	Ads_o
2 h	Infectivity (log PFU)	A	8.61 ± 0.14	8.33 ± 0.47
		B	8.61 ± 0.14	7.56 ± 0.31
	^{3}H-labeled RNA (log cpm)	A	3.58 ± 0.04	3.20 ± 0.46
		B	3.58 ± 0.04	3.19 ± 0.46
	^{14}C-labeled protein (log cpm)	A	3.41 ± 0.04	3.31 ± 0.67
		B	3.41 ± 0.04	3.27 ± 0.75
24 h	Infectivity (log PFU)	C	8.14 ± 0.17	7.74 ± 0.56
		D	8.14 ± 0.17	7.75 ± 0.72
	^{3}H-labeled RNA (log cpm)	C	3.74 ± 0.04	3.53 ± 0.35
		D	3.74 ± 0.04	3.67 ± 0.24
	^{14}C-labeled protein (log cpm)	C	3.18 ± 0.04	3.02 ± 0.48
		D	3.19 ± 0.04	2.87 ± 0.19

[a] Abbreviations: PFU, plaque-forming units; cpm, counts per minute.
[b] A, B and C, D are duplicates.

TABLE 3. *Comparison of virus initially adsorbed (Ads_i) on Al_2O_3 with virus recovered by kinetic analysis of data from four extractions (Ads_o)*

Incubation time	Measurement[a]	Sample[b]	Ads_i	Ads_i
2 h	Infectivity (log PFU)	A	9.90 ± 0.15	9.22 ± 0.94
		B	9.90 ± 0.15	8.60 ± 0.96
	^{3}H-labeled RNA (log cpm)	A	3.49 ± 0.04	3.43 ± 0.92
		B	3.49 ± 0.04	3.46 ± 0.86
	^{14}C-labeled protein (log cpm)	A	3.39 ± 0.04	3.46 ± 0.74
		B	3.39 ± 0.04	3.54 ± 0.80
24 h	Infectivity (log PFU)	C	10.03 ± 0.16	8.52 ± 1.88
		D	10.03 ± 0.16	7.86 ± 0.21
	^{3}H-labeled RNA (log cpm)	C	3.51 ± 0.04	3.24 ± 0.62
		D	3.51 ± 0.04	3.24 ± 0.69
	^{14}C-labeled (log cpm)	C	3.46 ± 0.05	3.28 ± 0.62
		D	3.46 ± 0.05	3.26 ± 0.74

[a] Abbreviations: PFU, plaque-forming units; cpm, counts per minute.
[b] A, B and C, D are duplicates.

TABLE 4. *Comparison of virus initially adsorbed (Ads_i) on MnO_2 with virus recovered by kinetic analysis of data from four extractions (Ads_o)*

Incubation time	Measurement[a]	Sample[b]	Ads_i	Ads_o
2 h	Infectivity (log PFU)	A	8.57 ± 0.22	7.53 ± 0.74
		B	8.57 ± 0.22	7.86 ± 0.21
	^{3}H-labeled RNA (log cpm)	A	2.93 ± 0.04	3.09 ± 0.24
		B	2.93 ± 0.04	3.06 ± 0.36
	^{14}C-labeled protein (log cpm)	A	3.14 ± 0.04	3.05 ± 0.18
		B	3.14 ± 0.04	2.97 ± 0.39
24 h	Infectivity (log PFU)	C	8.37 ± 0.30	7.13 ± 0.48
		D	8.37 ± 0.30	7.43 ± 0.29
	^{3}H-labeled RNA (log cpm)	C	3.73 ± 0.04	3.04 ± 0.30
		D	3.74 ± 0.04	3.02 ± 0.48
	^{14}C-labeled protein (log cpm)	C	3.15 ± 0.04	2.70 ± 0.43
		D	3.16 ± 0.04	2.68 ± 0.40

[a] Abbreviations: PFU, plaque-forming units; cpm, counts per minute.
[b] A, B and C, D are duplicates.

TABLE 5. *Comparison of virus initially adsorbed (Ads_i) on CuO with virus recovered by kinetic analysis of data from four extractions (Ads_o)*

Incubation time	Measurement[a]	Sample[b]	Ads_i	Ads_o
2 h	Infectivity (log PFU)	A	8.48 ± 0.21	7.52 ± 0.70
		B	8.48 ± 0.21	6.76 ± 0.53
	^{3}H-labeled RNA (log cpm)	A	2.91 ± 0.04	1.97 ± 0.66
		B	2.92 ± 0.04	1.97 ± 1.00
	^{14}C-labeled (log cpm)	A	3.09 ± 0.04	2.70 ± 0.29
		B	3.09 ± 0.04	2.60 ± 0.36
24 h	Infectivity (log PFU)	C	9.95 ± 0.19	6.24 ± 0.33
		D	9.95 ± 0.19	6.51 ± 0.39
	^{3}H-labeled RNA (log cpm)	C	2.91 ± 0.04	1.62 ± 0.89
		D	2.92 ± 0.04	1.76 ± 0.42
	^{14}C-labeled protein (log cpm)	C	3.11 ± 0.04	2.40 ± 0.35
		D	3.12 ± 0.04	2.40 ± 0.50

[a] Abbreviations: PFU, plaque-forming units; cpm, counts per minute.
[b] A, B and C, D are duplicates.

ing statistics and pipetting variation. Standard deviations about recovered amounts include scatter about linear regressions of C' data and minor variations in extraction volumes.

Kinetic plots for one of two 24-h samples, sample C in each case, are presented in Fig. 1 to 4. Concentrations for extraction data have been normalized by dividing each C' by the corre-

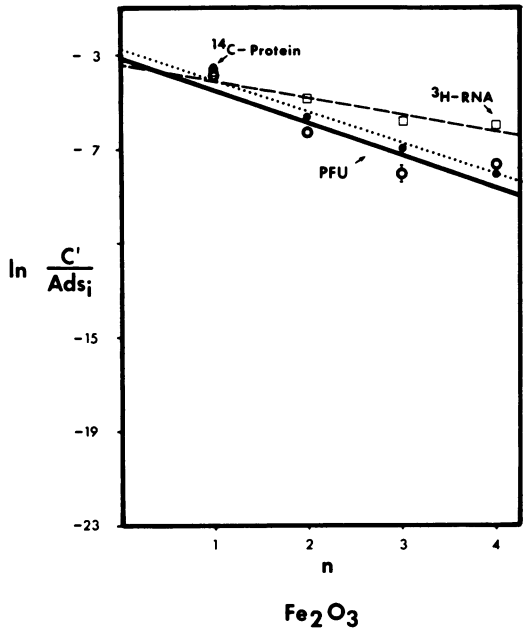

FIG. 1. *Kinetic plot of virus recovery with Fe_2O_3. Near coincidence of linear regression lines for plaque-forming units, ^{3}H-labeled RNA, and ^{14}C-labeled protein data suggests that the surface does not significantly inactivate virus.*

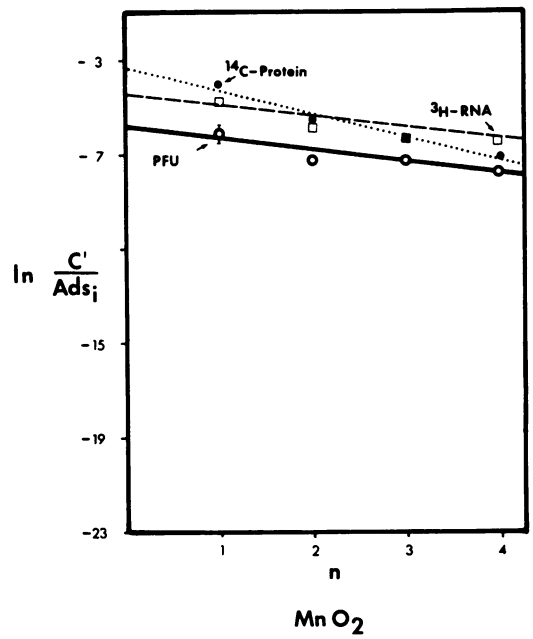

FIG. 3. *Kinetic plot of virus recovery with MnO_2. Significant inactivation is indicated by displacement of the regression line for infectivity data.*

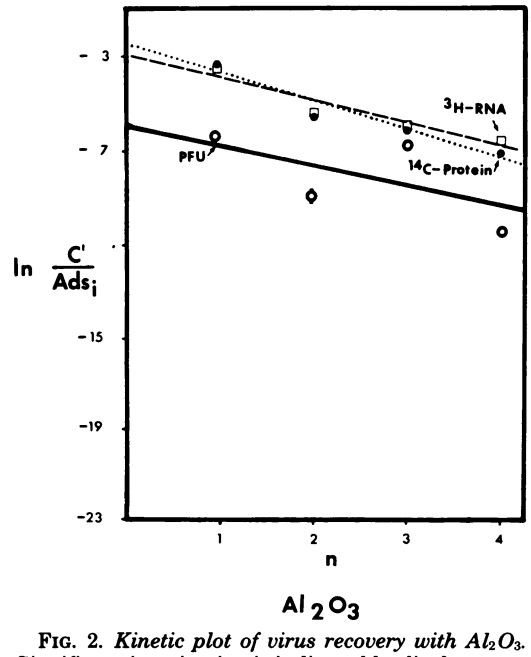

FIG. 2. *Kinetic plot of virus recovery with Al_2O_3. Significant inactivation is indicated by displacement of the regression line for infectivity data.*

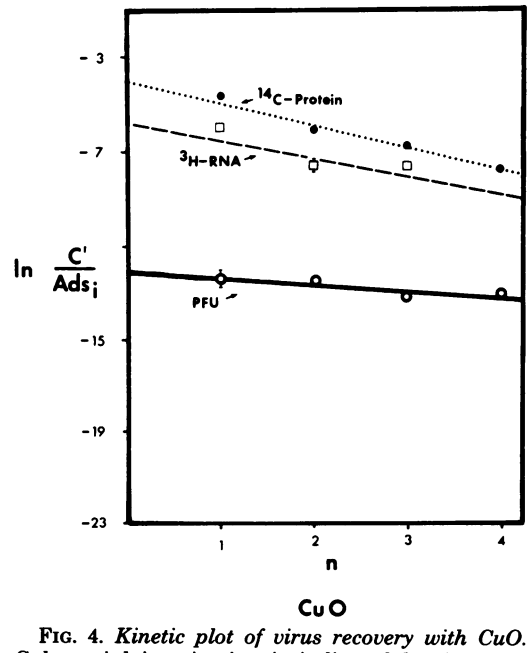

FIG. 4. *Kinetic plot of virus recovery with CuO. Substantial inactivation is indicated by the large displacement of the regression line for infectivity data.*

sponding Ads_i. If linear regressions of infectivity, ^{3}H-labeled RNA, and ^{14}C-labeled protein are coincident, and we have calculated that all of initially adsorbed material is recovered, virus is not inactivated. If normalized concentration plots show a decrease in infectivity data over radioactivity data, this suggests that virus is being inactivated. Conclusive demonstration of inactivation must also include comparison of recovered with initial infectivity and radioactivity. Statistical precision of plaque-forming unit data including pipetting error and random counting variation is indicated on the plots. For radioactivity data, analytical error is generally less than radii of plotted points.

With SiO_2, we recovered all infectivity and radioactivity in one extraction, and no inactivation was indicated. With Fe_2O_3 we recovered all radioactivity, but saw a minor loss of recoverable titer which may not be statistically significant. Linear regression lines for all three variables were nearly coincident and suggested a similar interpretation. On Al_2O_3 and MnO_2, we recovered nearly all initially adsorbed radioactivity except for 24-h MnO_2 samples, but observed significant decreases in infectivity. Regression lines of normalized plaque-forming unit concentration data plot below radioactivity data, also indicating inactivation.

With CuO, we saw a substantial loss in recoverable infectivity and a minor loss in recoverable radioactivity. Since the infectivity loss was considerably larger than the radioactivity loss, we have strong evidence that virus is substantially inactivated on the CuO surface. Kinetic plots also indicated substantial inactivation. In addition, regression lines for ^{3}H-labeled RNA and ^{14}C-labeled protein were substantially separated. This indicates that not only is the virus being inactivated, but it is being degraded by the CuO surface into fragments containing different amounts of RNA and protein which desorb differently. On aluminum metal (J. P. Murray and C. E. Schwerdt, manuscript in preparation), which degrades virus even more effectively than CuO, sedimentation analysis of degradation products indicates that desorbed degradation products are considerably smaller than infectious poliovirus RNA.

Variation of rate constant with extraction sequence number. An assumption in derivation of the kinetic theory presented earlier is that the desorption rate constant k does not significantly change during extractions. Variation of k could occur as a result of virus particle-particle interactions, i.e., virion clumping, or as a result of variation in the energy of virion-surface interaction with location on the solid surface. In the case where virus is degraded, it could occur as a result of differences in the surface interaction energy among whole virions and degradation products.

If the desorption rate is not constant, more easily desorbed material will leave the surface more rapidly than material that is less easily desorbed. The effect this will have on results obtained by application of our kinetic theory is that (i) concentration plots with extraction sequence number will exhibit a concave upward trend, and (ii) the total amount calculated to be recoverable will be smaller than the amount actually present on the surface.

With radioactivity data, we see a slight concave upward trend of the kinetic plots in most instances. This suggests that the desorption rate decreases slightly as we increase the number of extractions. In most cases, however, ^{3}H-labeled RNA and ^{14}C-labeled protein are completely recovered within the accuracy of our analysis. This suggests that errors introduced by our rate constant assumption are small. With plaque-forming unit data, statistical variation of titers is too large to detect possible non-linearity of kinetic plots.

Only on virus samples incubated with MnO_2 and CuO for 24 h do we see significant loss of recoverable radioactivity. We propose that this is due to differences in desorption rates in various degradation products. It could be that significant amounts of RNA and protein are denatured and are oriented on the surface in "random" coils interacting with the surface at a large number of points. This type of configuration could be very difficult to desorb.

DISCUSSION

Mechanism of degradation. Ginoza (5) presents considerable evidence that viruses are thermodynamically unstable as they spontaneously inactivate at finite temperature-dependent rates at ambient temperatures. Korant and Lonberg-Holm (presented at the 1977 Annu. Meet. Am. Soc. Microbiol., New Orleans, La.) view picornaviruses as "cocked and ready to be triggered to undergo a profound conformational alteration ... leading to irreversible loss of infectivity when alteration occurs prematurely."

Adsorption to and elution from host cells has been shown to reduce the specific infectivity of adsorbed poliovirus preparations. Altered virions are not able to reattach. In addition, both heat-shocked virions (8) and virions adsorbed to and eluted from host cells (4) are partially disassembled.

Aluminum metal (Murray and Schwerdt, manuscript in preparation) and transition metal oxides are certainly more effective in degrading virus than silica. Aluminum metal appears to be

considerably more effective in adsorbing virus than Al_2O_3 (Murray and Parks, manuscript in preparation). The strong Van der Waals interactions (13) thought to be responsible for the increased tendencies of metals and transition metal oxides to adsorb viruses may well be involved in catalyzing spontaneous degradation. This is consistent with the observation that human erythrocytes are more readily hemolyzed by Zn metal than ZnS or ZnO (3). Specific inactivation of myosin adenosine 5'-triphosphatase on SiO_2 surfaces (10) suggests that with some materials, mechanisms involving catalysis by atoms in surface sites could be involved however, rather than interactions developed in the bulk solid.

Our recovery data indicate that virus is rapidly inactivated at first and proceeds more slowly after 2 h. This is inconsistent with a simple inactivation model where the rate of inactivation is defined by a first-order reaction with respect to the concentration of adsorbed virions. Heterogeneity in site reactivities, virion clumping, or the possibility that inactivation occurs mostly at impact and is therefore predominantly a function of virion concentration in solutions could account for observed inactivation rates.

Virus inactivation and degradation by reactive inorganic surfaces may prove to be an important mechanism limiting the dissemination of viruses in soil and aquatic environments. In some cases, however, virus may actually be protected by adsorption, as Mitchell and Jannasch (11) and Smith et al. (12) suggest from their studies of virus inactivation rates in seawater in the presence of suspended sediments.

Techniques developed for this study are applicable to many other systems, e.g., alteration of enzymes by adsorption to various materials. In addition, they can be readily applied to recovery problems such as obtaining accurate measures of total virus adsorbed to soil samples or virus recovery from solids used for concentration procedures in analysis of contaminated water.

ACKNOWLEDGMENTS

C. E. Schwerdt, G. A. Parks, and H. H. Huang are thanked for laboratory space and helpful comments. S. Enriquez, M. R. Sanchez, and E. Terehoff are thanked for technical assistance.

This project was funded by grant R-805016-01 from the U.S. Environmental Protection Agency.

LITERATURE CITED

1. **Brunauer, S., P. Emmet, and E. Teller.** 1938. The adsorption of gasses in multimolecular layers. J. Am. Chem. Soc. **60**:309-319.
2. **Charney, J., R. A. Machlowitz, and D. S. Spicer.** 1962. The adsorption of poliovirus antigen to glass surfaces. Virology **18**:495-497.
3. **Delbeck, G., and M. Delbeck.** 1973. Hämolyse und Hämoglobinadsorption durch Zinkverbindungen. Res. Exp. Med. **160**:255-260.
4. **Fenwick, M. L., and P. D. Cooper.** 1962. Early interactions between poliovirus and ERK cells: some observations on the nature and significance of the rejected particles. Virology **18**:212-223.
5. **Ginoza, W.** 1968. Inactivation of viruses by ionizing radiation and by heat, p. 139-209. *In* K. Maramorosch and H. Koprowski (ed.), Methods in virology, vol. 4. Academic Press Inc., New York.
6. **Hill, W. F., Jr., E. W. Akin, and W. H. Benton.** 1971. Detection of viruses in water: a review of methods and application, p. 17-24. *In* V. Snoeyink and V. Griffin (ed.), Proceedings of the Thirteenth Water Quality Conference—Virus and Water Quality: Occurrence and Control, vol. 69. University of Illinois, Urbana.
7. **Joklik, W. K., and J. E. Darnell, Jr.** 1961. The adsorption and early fate of purified poliovirus in HeLa cells. Virology **13**:439-447.
8. **Jordan, L., and H. D. Mayor.** 1974. Studies on the degradation of poliovirus by heat. Microbios **9**:51-60.
9. **McClain, M. E., and C. E. Schwerdt.** 1954. Use of HeLa cells for plaque assay of poliomyelitis virus. Fed. Proc. Am. Soc. Exp. Biol. **13**:505.
10. **Matsumura, Y., and T. Matsumura.** 1972. Inactivation of myosin ATPase by condensed polysilicic acid powders. J. Biochem. (Tokyo) **71**:711-717.
11. **Mitchell, R. W., and H. W. Jannasch.** 1969. Processes controlling virus inactivation in seawater. Environ. Sci. Technol. **3**:941-943.
12. **Smith, E. M., C. P. Gerba, and J. L. Melnick.** 1978. Role of sediment in the estuarine environment. Appl. Environ. Microbiol. **30**:212-222.
13. **Visser, J.** 1976. Adhesion of colloidal particles, p. 3-84. *In* E. Matijevic (ed.), Surface and colloid science, vol. 8. John Wiley, New York.